

The application of texture measures to classifying the rain forest

CHRIS OLIVER

DERA, St Andrew's Road, Malvern, Worcs., WR14 3PS, UK.
chris@sar.dera.gov.uk

Abstract. This paper describes the application of SAR texture in classifying examples of Amazon rain forest into *forest* and *not forest* categories. The results are compared with corresponding classification of Band 5 Landsat TM imagery.

Keywords: remote sensing, SAR, texture classification.

1 Introduction

A typical SAR image of the Tapajos region of the Amazon rain forest is shown in Figure 1. This was obtained with the Canadian Centre for Remote Sensing C-band airborne system in 1992 as part of the SAREX-92 campaign. The Santarem-Cuiaba highway is visible running from the top right to bottom left of the image. The area to the left of this highway is in the Tapajos National Park and so comprises almost entirely primary rain forest. To the right of the highway there is a mixture of primary forest and clearings, some with different degrees of regeneration. Note that the return from primary rain forest shows greater fluctuations than from secondary forest, including both clearings and regions of regeneration [1-4].

The observed texture of primary forest has been shown to be reasonably consistent with a K-distributed intensity or amplitude arising from combining an underlying gamma-distributed RCS fluctuation with speckle during the imaging process [1,2,4]. Previous studies [5-7] demonstrated that the normalised log texture measure, defined by $U_x \equiv \ln \bar{x} - \overline{\ln x}$, approximates the optimum estimator for determining the order parameter of K-distributed radar clutter, where the bars represent local averages over a window of M pixels. As the number of looks increases this measure tends to the full Maximum Likelihood Estimator as the PDF converges on a gamma-distribution. Such texture is characterised completely by the mean, m , and order parameter, n , of the distribution. Residual fluctuations in the texture measure due to speckle can then be removed using simulated annealing [3,4]. Indeed, the texture can be classified by applying a threshold corresponding to an order parameter value of about 3 [1,4]. In Section 2 we segment the SAR image using annealing methods [8-10] followed by classification achieved by applying a threshold to the segmented texture [10].

It is essential that classification based on this SAR texture should be compared with current techniques using Landsat TM optical imagery. The Landsat TM imagery used in the comparison was gathered on 29/07/92 with a resolution of 30m. It has been demonstrated to give visually reasonable classification using the Band 5 (approximately 1 μ m) image [11-13]. We shall adopt

© British Crown Copyright, DERA/1998

Published with the permission of the Controller of Her Britannic Majesty's Stationery Office



Figure1: SAREX-92 image of part of the Tapajos rain forest in Amazonia.

this imagery for a reference classifier in the present study.

Initially, in Section 2, we adopt a simple test scene containing two dominant regions, corresponding to primary forest and clearing, denoted as *forest* and *not forest* respectively. This scene can be used to compare classification performance in regions of simple structure. We combine an optimised texture measure with annealed segmentation methods to assign the image into these two categories. These results are then compared with corresponding classification derived from the Landsat TM Band 5 image of the same area, following annealed intensity segmentation. Finally, in Section 3, we apply the technique to the SAREX-92 scene in Figure 1, previously studied in the development of texture analysis methods [3,4], and examine the degradation in performance as more complicated land-use structures are encountered.

2 Classification of test scene

Initially we apply annealed texture segmentation to a simple test image covering about 1.8×1.8 km extracted from SAREX-92 data. The image, illustrated in Figure 2(a), is dominated by single regions of *forest* and *not forest* classes. The first stage in texture analysis is to form the normalised log estimate over a 12×12 pixel window, as shown in Figure 2(b). It is obvious that the area of uniform texture, arising from the *not forest* region, yields small values of texture measure, corresponding to large values of order parameter, $n \geq 5$. The region of primary forest shows considerably more variation with large values of the texture measure, corresponding to $n \approx 1$ [4]. However, there is still fluctuation in the data, due to the original speckle, which can be reduced using annealing methods [3,4].

When we apply an annealed segmentation algorithm [8,9] to the texture in Figure 2(b) the result illustrated in Figure 2(c) is obtained. The final stage in classification is to apply a single threshold to Figure 2(c) in order to discriminate between the two classes. An order parameter value of about 3 is expected to provide a suitable classification [1,4]. The region boundary identified by threshold detection is then overlaid on the original image in Figure 2(d). It is clear that the algorithm has provided a reasonable classification of the SAR texture. The primary forest region has a narrow bright strip on its leading edge, caused by the radar illumination. This is correctly identified as part of the *forest* class. There also appears to be a small region of increasing texture, presumably corresponding to regeneration, at the top of the *not forest* region which has been included in the *forest* category. This visual comparison is only qualitative; quantitative testing can only take place when the results are compared with those from the TM data.

Annealed intensity segmentation is applied to the equivalent Band 5 ($1 \mu\text{m}$) Landsat TM image the original image followed by a threshold to discriminate between the two classes. The TM region boundary is overlaid onto the original TM image in Figure 2(e). As a visual demonstration of the close agreement between the classifications we overlay the TM boundary on the SAR classes in Figure 2(f). Though there are detailed differences along the boundary region, these only represent a small fraction of the pixels assigned to the two classes.

Let us denote the TM classifications as F and NF for *forest* and *not forest* classes respectively, with f and nf denoting the equivalent SAR classes. The performance can then be summarised in terms of the conditional probabilities $P(f|F)$ and $P(nf|NF)$. Optimum accuracies of 97.8% and 96.5% are achieved for these probabilities when a threshold corresponding to $n \approx 3.5$ is applied to the SAR texture. This demonstrates that the methods based on SAR texture and TM intensity lead to very similar performance for the simple test scene chosen.

3 Classification of mixed scene

Let us therefore now apply the same algorithms to the SAREX-92 scene measuring about 9×9 km shown in Figure 1. This has a large fraction of regenerating forest, unlike the test area. Newer areas of regrowth should be classified as *not forest* whereas older areas would begin to resemble primary forest and be classified accordingly. The TM threshold remains unchanged from the test scene. However, the texture threshold needs to be reduced below $n = 3.5$ to achieve better *not forest* detection in regenerating regions. In consequence, there is an increased probability of

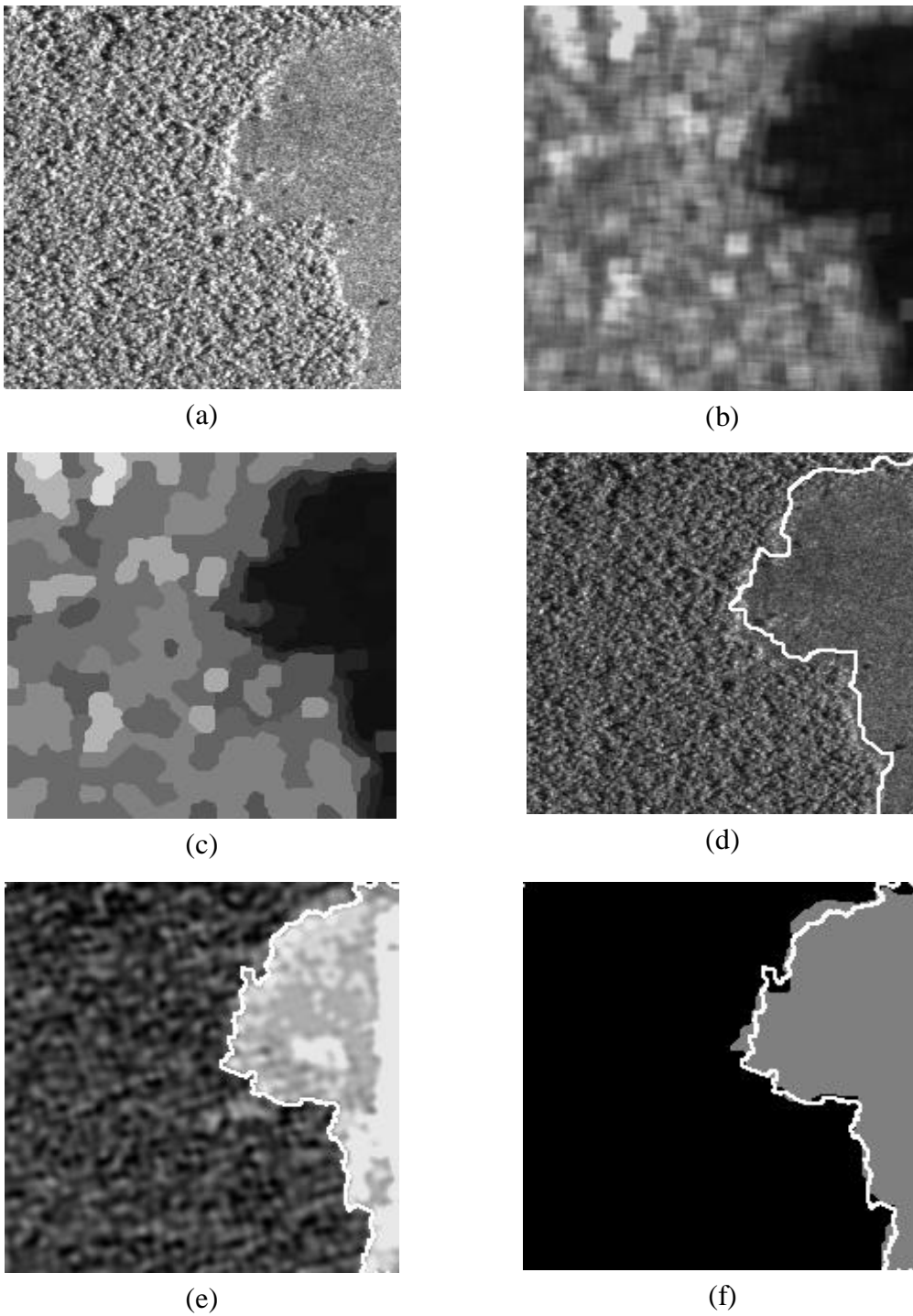


Figure 2: Analysis of the test scene; (a) original SAR image, (b) normalised log measure over 12×12 window, (c) result of applying annealed segmentation to (b), (d) overlay of SAR region boundary on SAR image, (e) overlay of corresponding TM region boundary on TM image, (f) overlay of TM class boundary on SAR class.

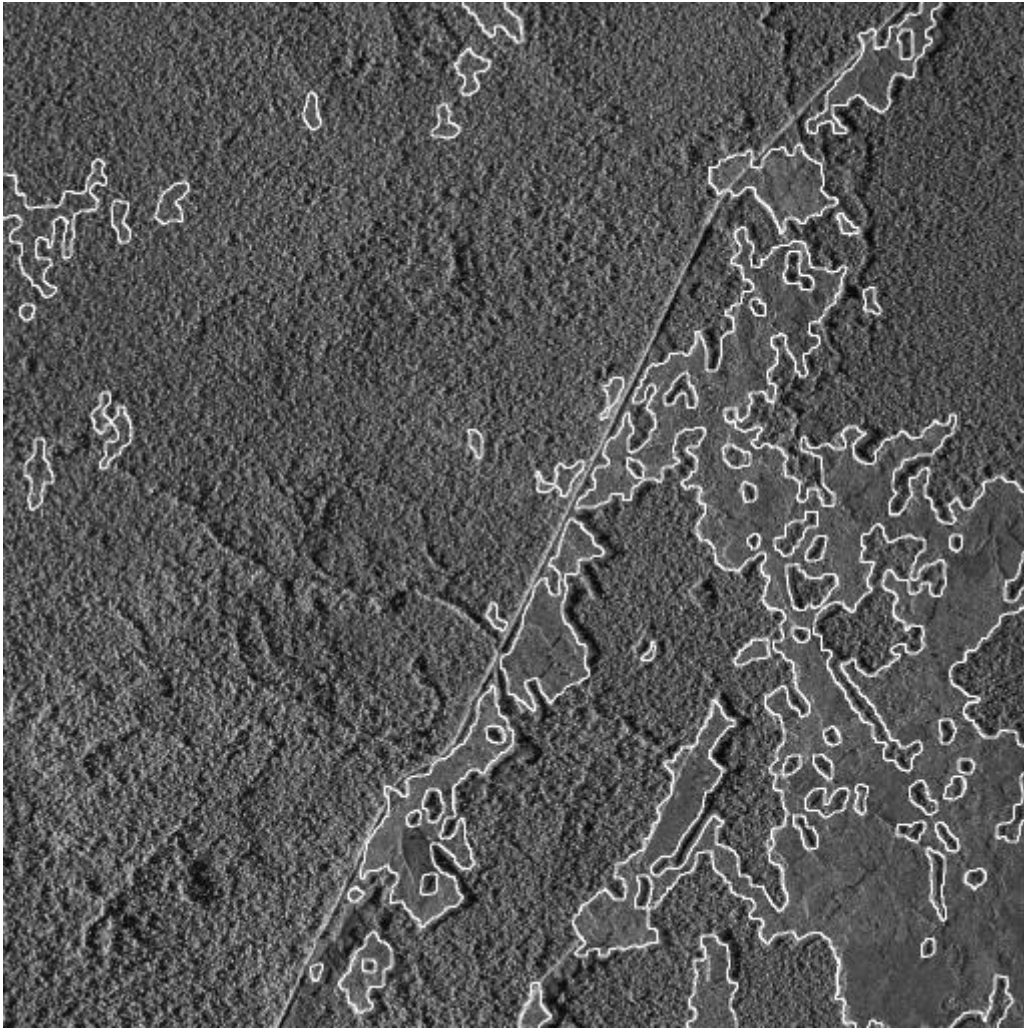


Figure 3: Overlay of SAR class boundary on original SAR image of Figure 1.

misclassifying *forest* regions as *not forest*. This behaviour is clearly visible in the top left hand quarter of Figure 3, which illustrates an overlay of the boundary between *forest* and *not forest* classes determined from the SAR texture on the original SAR image. The equivalent result for TM data, illustrated in Figure 4, contains only 0.15% of *not forest*. As a compromise between improved *not forest* detection and acceptable false alarms, a threshold corresponding to $n = 2.6$ was adopted for the SAR texture which is used in all subsequent analysis. It yields a 4.3% (false) detection probability for the top left region. Note that these incorrectly classified *not forest* regions in the top left quarter appear less textured than their surroundings, though they are not thought to be real clearings, or even regenerating regions. The probability that regenerating regions are not detected from the SAR texture can be evaluated from the bottom right quarter of the scene which consists of 49.3% *not forest*, largely made up of regenerating regions. The corresponding classification rate from the SAR data is 46.1%.

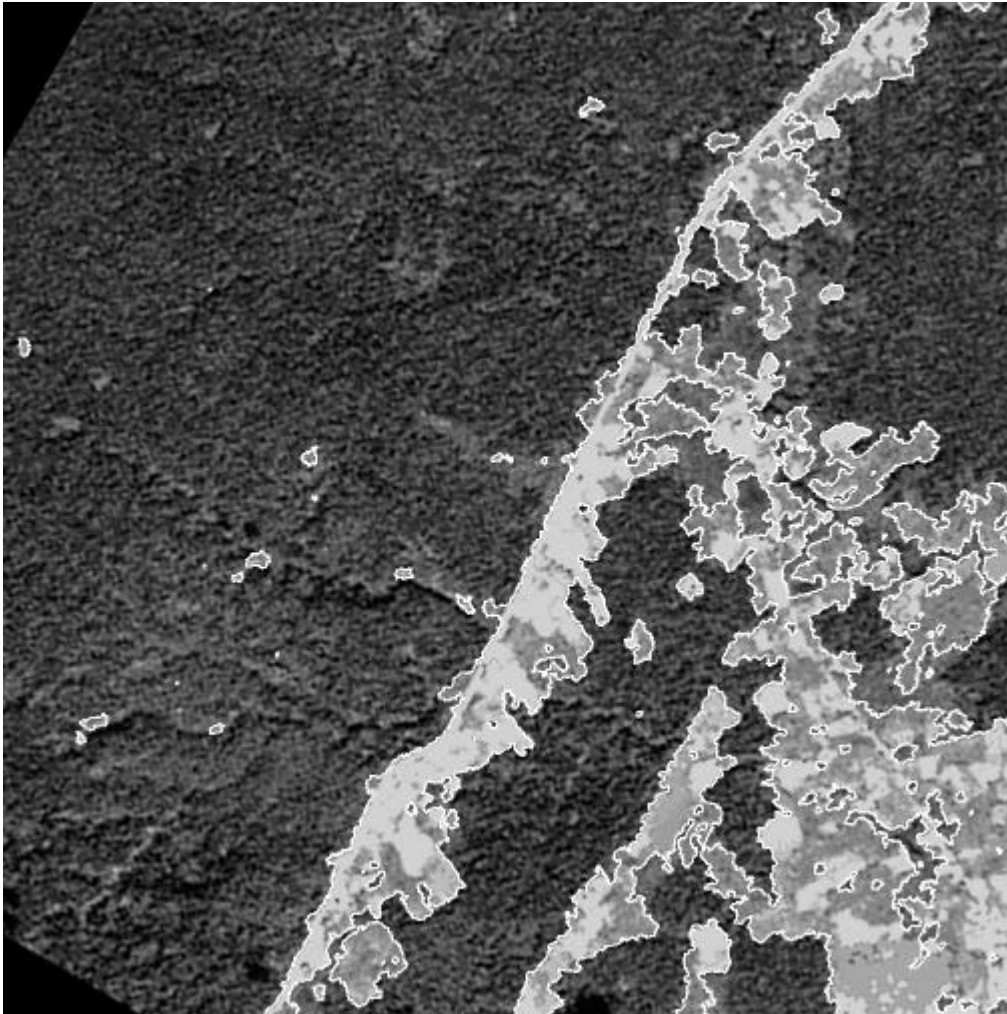


Figure 4: Overlay of TM class boundary on original TM image of the same scene as Figure 1.

On comparing Figures 3 and 4 there are two distinct structural differences in the way in which the SAR and TM classifiers operate. Firstly, on the left hand edge of the extended region of clearings along the highway, the SAR *not forest* class is displaced to the right in Figure 3. This is because the TM classification includes the highway, which is a bright feature in Figure 4, as part of the *not forest* class. The SAR texture incorrectly classifies it as *forest* since there is a strong variation in cross-section. However, in principle, the position of such a highway is known a priori and suitable correction should be made, as we discuss later. Secondly, the right hand edge of *not forest* regions from the SAR texture is generally displaced to the left of the TM boundary. This is because the SAR texture classifier incorrectly interprets the high-contrast shadows following *forest* regions as *forest*. On the other hand, the left hand side of each clearing displays a bright high-contrast region because of the illumination of the front edge of the primary forest, which is correctly classified as *forest*. The failure to assign shadowed regions correctly reduces the area classified as *not forest* from SAR compared with TM. Contextually, the high contrast shadow

region always lies between primary forest and clearing and so can be identified from the texture and the resulting additional (shadow) area added to the *not forest* class.

For a final illustration we compare the SAR (following correction for shadowing) and TM classifications in Figure 5. The two-element classified regions from the SAR texture are shown with black denoting *forest* and grey *not forest* regions. The overlay corresponds to the boundaries of the two classes derived from the TM data. Though the general features of the two classifications are broadly similar, there are significant discrepancies which we now discuss in terms of the quantitative performance. This is summarised separately for each of the four quarters of the image, as well as for the complete scene, in Table 1. The results include the effect of correction for shadowing which increases the probability of detecting a *not forest* region by about 10% over the whole image. Scenes with less structure would not require such a large correction.

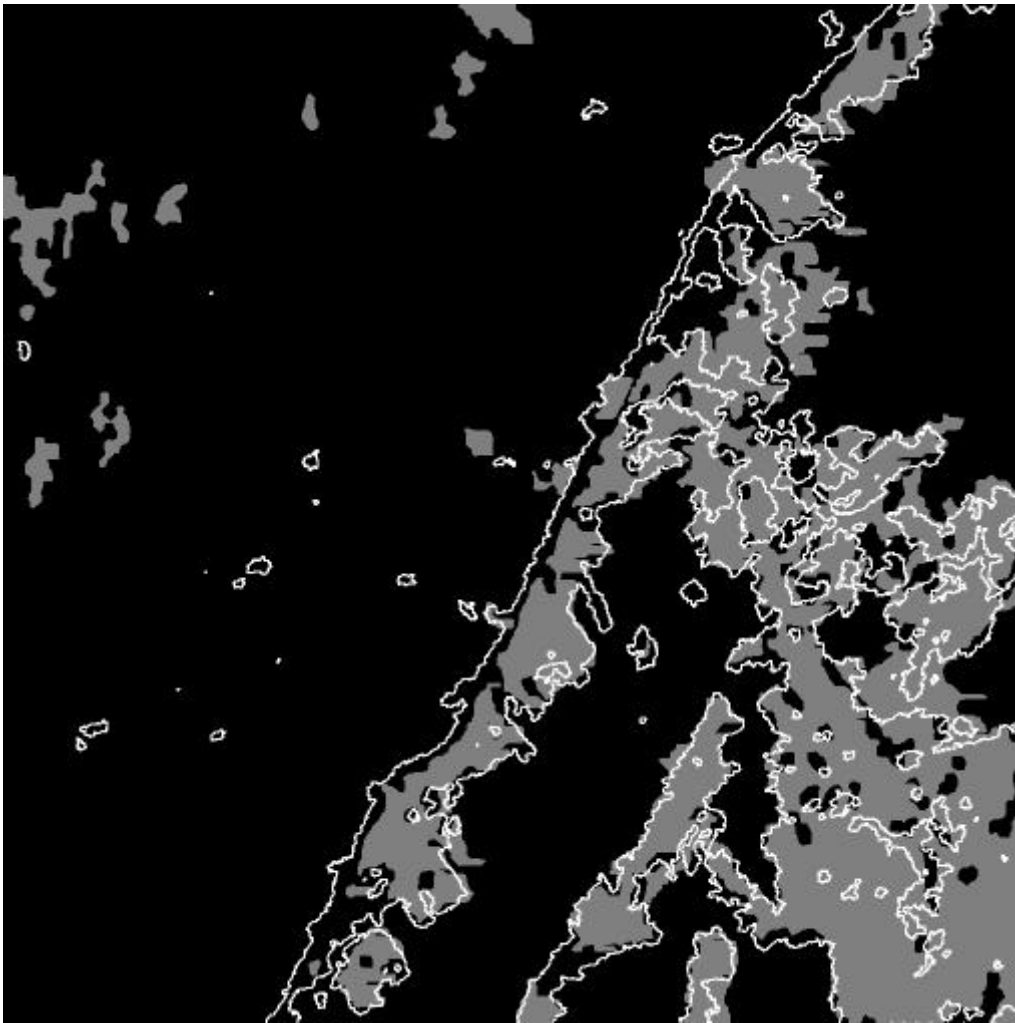


Figure 5: Overlay of the TM class boundary on the SAR class after correction for shadowing.

Image	$P(NF)$	$P(nf)$	$P(nf NF)$	$P(f F)$
top left	0.0015	0.046	0	0.954
top right	0.192	0.213	0.627	0.885
bottom left	0.110	0.064	0.516	0.992
bottom right	0.493	0.488	0.803	0.819
complete	0.199	0.203	0.721	0.925

Table 1: Summary of the corrected classification performance in the different image quarters as well as the complete scene.

The number of pixels incorrectly classified from the SAR texture as *not forest* in the top left quarter has controlled the selection of the texture threshold as described above. The top right quarter has similar overall probabilities of detecting *not forest* regions with both sensors. However, the conditional probability $P(nf|NF)$ is only 63% after correction, which reveals that there is a large discrepancy between regions thus classified. The SAR texture only yields half the probability for detecting *not forest* regions of that for the TM data in the bottom left quarter. The corresponding conditional probability is reduced by a similar amount. Both sensors yield similar *not forest* classification probability in the bottom right quarter. The conditional probabilities for both *not forest* and *forest* show that similar fractions of *not forest* and *forest* pixels are misclassified. Finally, the classification performance for the whole image reveals a high level of misclassification in the scene when compared with the excellent performance obtained with the test scene.

Let us now identify the causes of the observed misclassification by examining the details of the results in Figures 3 to 5 in addition to the classification probabilities in Table 1.

- a) In the primary rain forest to the left of the highway both SAR and TM classification yield non-overlapping *not forest* regions which are false alarms arising from statistical fluctuations in the local properties. The corresponding classification accuracy for *not forest* is then very small with $P(nf|NF) \approx 0$.
- b) The discrepancy in classifying the highway, noted earlier, has a considerable impact on performance. The average width of the clearing surrounding the highway is about 16 pixels (144m). The additional area belonging to the *not forest* class would then be 1.6% of the image. If these pixels are removed from the comparison, the conditional probability of correctly

classifying *not forest* regions would increase to 78% from 72%. The correction in each quarter of the image would differ, resulting in an increase from 63% to 73% on the top right, 52% to 72% on the bottom left and 80% to 81% on the bottom right. As noted earlier, this effect could be predicted from knowledge of the highway position.

- c) The main residual discrepancy is then associated with the existence of regenerating regions, particularly noticeable in the top right quarter of the scene. Though both sensors yield similar total areas in each class, the overlap between the classifications is poor, with $P(nf|NF) = 0.627$. However, it should be noted that in regions where the SAR texture has resulted in a *not forest* classification, the TM data often shows evidence that these regions possibly differ from the true *forest* class, though not enough to affect the classification. There are also regions in which the brightness of the TM image is sufficient for an area to be identified as being *not forest* where the SAR image shows cross-section fluctuations which place it in the *forest* category.
- d) Comparison of Figures 3 and 4 suggest that the *not forest* class in the bottom right quarter of the scene is largely made up of regenerating regions rather than actual clearings. This region was considered in the selection of an appropriate texture threshold for including regenerating regions in the *not forest* class. The *not forest* classification accuracy within this region is increased to $P(nf|NF) = 0.803$ compared to the other quarters with a similar *forest* classification accuracy of $P(f|F) = 0.819$, when the small correction for the highway is ignored. These results are still considerably poorer than the earlier comparison on the test scene because of contributions from all the effects in a) to c).

4 Conclusions

This comparison of rain forest classification using SAR texture and Landsat TM Band 5 intensity, has shown a high degree of similarity where a two-element classification into *forest* and *not forest* is performed on regions which are differentiated into primary forest and clearing. The probability of both sensors yielding *forest* and *not forest* classifications were found to be 97.8% and 96.5% respectively with an order parameter threshold of 3.5. This shows that SAR texture can be a very powerful discriminant in the identification of new clearings in primary forest.

When the scene includes regions of regenerating secondary forest, the texture threshold has to be reduced to 2.6 to improve the classification of regenerating regions as *not forest*. When the large regions of shadow associated with the forest edge are identified separately and appropriate correction made the accuracy of classification becomes 92.5% and 72.1% for *forest* and *not forest* respectively. A second contribution to degraded performance arises from the region around the highway. We have shown that the *not forest* detection probability should be increased to about 78% if the area occupied by the clearing around the highway is eliminated from the comparison. The performance is still considerably poorer than for the test scene, largely as a consequence of the different manner in which the sensors respond to regenerating regions. This physical difference cannot be overcome by any modifications to this approach. Indeed, it is not really possible to claim that either sensor is giving a 'correct' classification without detailed ground truth. In spite of these limitations, the existing approach will already be effective where there are large regions of each class, so that structural effects do not dominate, and where we are primarily concerned with detecting the presence of new clearings within the rain forest.

References

1. Yanasse C C F, Frery A C, Sant'Anna S J S, Filho P H and Dutra L V, 'Statistical Analysis of SAREX data over Tapajos - Brazil', Final results Workshop for SAREX '92, Paris, 1993, pp. 1-16.
2. Grover K D and Quegan S, 'Image quality, statistical and textural properties of SAREX data from the Tapajos test site', *Proc. SAREX-92 Workshop*, ESA WPP-76, 1994, pp. 15-23.
3. Oliver C J, Blake A P and White R G, 'Optimum texture analysis of SAR images', *Proc. SPIE Conf. Algorithms for Synthetic Aperture Radar Imagery, Orlando, Florida*, **Vol. 2230**, 1994, pp. 389-398.
4. Oliver C J, 'Edge detection in SAR segmentation', *Proc. Europto Conf. on SAR Data Processing for Remote Sensing, Rome*, **Vol. 2316**, 1994, pp. 80-91.
5. Oliver C J, 'Optimum texture estimators for SAR clutter', *J. Phys. D: Appl. Phys.*, **Vol. 26**, 1993, pp. 1824-1835.
6. Blacknell D, 'A comparison of parameter estimators for the K distribution', *IEE Proc. Radar, Sonar, Navig.*, **Vol. 141 (1)**, 1994, pp. 45-52.
7. Lombardo P and Oliver C J, 'Estimation of texture parameters in K-distributed clutter', *IEE Proc. Radar, Sonar, Navig.*, **Vol. 141 (4)**, 1994, pp. 196-204.
8. Oliver C J, McConnell I and Stewart D, 'Optimum texture segmentation of SAR clutter', 1996, *Proc. EUSAR 96, Konigswinter*, pp. 81-84.
9. Cook R, McConnell I, Stewart D and Oliver C J, 'Segmentation and simulated annealing', *Europto Conf. on SAR image analysis, simulation and modelling II, Taormina, Italy*, **Vol. 2958**, 1996, pp. 30-37.
10. Oliver C J and Quegan S, 'Understanding Synthetic Aperture Radar Images', 1998, Artech House: Boston.
11. Boyd D S, Foody G M, Curran P J, Lucas R M and Hanzak H, 'An assessment of radiance in Landsat TM middle and thermal infrared wavebands for the detection of tropical forest regeneration', *Int. J. Remote Sensing*, vol. 17, 1996, pp. 249-261.
12. Grover K D, 'Studying forestry in Brazilian Amazonia using Synthetic Aperture Radar', PhD Thesis, Dept. of Applied and Computational mathematics, University of Sheffield, 1995.
13. Grover K D, Quegan S and Yanasse C C F, 'Quantitative estimation of tropical forest cover by SAR', *IEEE Trans. Geosci. Remote Sensing*, 1998, to be published.